MIT Libraries | DSpace@MIT

MIT Open Access Articles

Unsteady Flow and Whirl-Inducing Forces in Axial-Flow Compressors: Part II—Analysis

The MIT Faculty has made this article openly available. ***Please share*** how this access benefits you. Your story matters.

Citation: Ehrich, F. F. et al. "Unsteady Flow and Whirl-Inducing Forces in Axial-Flow Compressors: Part II—Analysis." Journal of Turbomachinery 123.3 (2001): 446. © 2001 by ASME

As Published: http://dx.doi.org/10.1115/1.1370165

Publisher: ASME International

Persistent URL: http://hdl.handle.net/1721.1/106282

Version: Final published version: final published article, as it appeared in a journal, conference proceedings, or other formally published context

Terms of Use: Article is made available in accordance with the publisher's policy and may be subject to US copyright law. Please refer to the publisher's site for terms of use.

Massachusetts Institute of Technology

2000 Turbomachinery Committee and Structures & Dynamics Committee Best Paper Award

Unsteady Flow and Whirl-Inducing Forces in Axial-Flow Compressors: Part II—Analysis

F. F. Ehrich
Z. S. Spakovszky
M. Martinez-Sanchez
Massachusetts Institute of Technology, Cambridge, MA 02139

S. J. Song
Seoul National University, Seoul, Korea

D. C. Wisler
A. F. Storace
H.-W. Shin
B. F. Beacher
GE Aircraft Engines, Cincinnati, OH 45215

An experimental and theoretical investigation was conducted to evaluate the effects seen in axial-flow compressors when the centerline of the rotor becomes displaced from the centerline of the static structure of the engine, thus creating circumferentially nonuniform rotor-tip clearances. This displacement produces unsteady flow and creates a system of destabilizing forces, which contribute significantly to rotor whirl instability in turbomachinery. These forces were first identified by Thomas (1958. Bull. AIM, **71***, No. 11/12, pp. 1039–1063.) for turbines and by Alford (1965. J. Eng. Power, Oct., pp. 333–334) for jet engines. In Part I, the results from an experimental investigation of these phenomena were presented. In this Part II, three analytic models were used to predict both the magnitude and direction of the Thomas/Alford force in its normalized form, known as the β coefficient, and the unsteady effects for the compressors tested in Part I. In addition, the effects of a whirling shaft were simulated to evaluate differences between a rotor with static offset and an actual whirling eccentric rotor. The models were also used to assess the influence of the nonaxisymmetric static pressure distribution on the rotor spool, which was not measured in the experiment. The models evaluated were (1) the two-sector parallel compressor (2SPC) model, (2) the infinite-segment-parallel-compressor (ISPC) model, and (3) the two-coupled actuator disk (2CAD) model. The results of these analyses were found to be in agreement with the experimental data in both sign and trend. Thus, the validated models provide a general means to predict the aerodynamic destabilizing forces for axial flow compressors in turbine engines. These tools have the potential to improve the design of rotordynamically stable turbomachinery.*
[DOI: 10.1115/1.1370165]

1 Introduction

It is critically important to the operation of high-bypass ratio, turbofan engines and other high-speed, highly loaded turbomachinery that their rotor systems be designed to preclude potentially destructive rotordynamic instability. Instability is engendered when whirl-inducing tangential force systems are induced by radial deflection of the rotor, i.e., cross-coupled forces, with a magnitude that overwhelms stabilizing damping forces. Typical mechanisms for inducing such forces are those associated with internal damping of the rotor (hysteretic whirl); with fluid film bearings; with fluid trapped in internal cylindrical cavities in rotors; and, as addressed in this paper, with the system of aerodynamic forces induced by the nonaxisymmetric rotor and stator tip clearances inherent in rotor displacement. It is therefore of major importance in the design process to be able to determine accurately the magnitude and direction of these whirl-inducing forces.

The aerodynamic forces induced by the nonaxisymmetric rotor and stator tip clearances inherent in rotor displacement were first identified by Thomas [1] for turbines and by Alford [2] for jet engines for both compressors and turbines. Vance and Laudadio [3] found that the Thomas/Alford force is rotor-speed dependent and mostly positive, except for some special combinations of rotor speed and stage torque where the direction of the force was reversed. Colding-Jorgensen [4] found the same generality for the shape and slope of the relationship of β coefficient versus flow coefficient as later reported by Ehrich [5], but the Colding-Jorgensen results suggested a more positive level of the parameter than the negative levels reported in Ehrich's work. Ehrich [5] further showed that the experimental data of Vance and Laudadio [3] implied that, for certain values of torque and speed in their low-speed blower tests, the destabilizing forces tend to drive backward whirl. Other evidence was also accumulating in the theoretical and experimental results of Yan et al. [6] to indicate negative β coefficients for compressors.

A key limitation to the application of the new insights into the destabilizing forces in axial-flow compressors was the lack of accurate, systematic, experimental data that could be used to validate the available analytic procedures. Part I of this two-part paper presents experimental results from several compressor configurations that accurately model compressors in commercial airline service. The tests, conducted in the GE Aircraft Engine's low-speed research compressor (LSRC), used rotor centerline offset to simulate the amplitude of rotor whirl and provide the opportunity to measure the major destabilizing forces that are induced.

2 Objectives

There were two major objectives of this overall work. The first was to compare the available analytic models with the experimental results to validate their potential incorporation into design systems. The second was to assess the relative importance of two effects that were not evaluated in the experimental program—the effects of a whirling shaft, which was not simulated by the static

Contributed by the International Gas Turbine Institute and presented at the 45th International Gas Turbine and Aeroengine Congress and Exhibiton, Munich, Germany, May 8–11, 2000. Manuscript received by the the International Gas Turbine Institute February 2000. Paper No. 2000-GT-566. Review Chair: D. Ballal.

 Copyright © 2001 by ASME

Downloaded From: http://turbomachinery.asmedigitalcollection.asme.org/ on 10/24/2016 Terms of Use: http://www.asme.org/about-asme/terms-of-use

offset used in the experiment; and the influence of the nonaxisymmetric static pressure distribution on the rotor spool, which was not measured in the experiment.

3 Description of the Three Analysis Methods

The predictions of three analytic systems were compared in detail to the experimental results that were obtained in Part I. The three methods vary from one another in several ways: (a) in their dependence on experimental characterization of the stage; (b) in their flexibility in dealing with configuration detail like shrouded blade rows; (c) in their accuracy of prediction of the β coefficient compared to the experimental data; and (d) in their capability to accommodate more complex phenomena like the effects of nonaxisymmetric spool surface pressure and of the whirling rotor on the β coefficient.

3.1 Two-Sector-Parallel-Compressor Model. Ehrich [5] developed a procedure, referred to as the two-sector-parallel-compressor model (2SPC), which computes the β coefficient based on parallel compressor theory. The 2SPC model is a one-dimensional system that approximates the continuous circumferential variation of clearance by hypothesizing two compressors operating in parallel, one representing a 180 deg sector with an axisymmetric clearance equal to the minimum local clearance of the deflected rotor; and the other compressor representing the other 180 deg sector with an axisymmetric clearance equal to the maximum local clearance of the deflected rotor. The analysis requires only the stage performance characteristics at two values of axisymmetric tip and/or shroud seal clearance. The model is not able to offer any data or insight on other effects such as actual whirling of the rotor or the effect of nonaxisymmetric pressure distribution on the rotor spool.

3.2 Infinite-Segment-Parallel-Compressor Model. More recently, Spakovszky [7] developed a new procedure, referred to here as the infinite-segment-parallel-compressor model (ISPC), which consists of two parts: (a) an unsteady, two-dimensional, compressor tip clearance model for stall inception, which represents the flow field through the compressor, and (b) a rotordynamic force model. The rotordynamic model uses the unsteady momentum equation, which is applied locally to one blade passage in the circumferential direction. An unsteady control volume analysis is conducted in a frame locked to the rotor and applied locally to each blade passage to obtain the local tangential blade force. The resulting force in the rotor frame, which is obtained by integrating the distributed tangential force, is transformed back to the absolute frame. One advantage of this approach over that of the 2SPC model is that any unsteady flow regime (whirling shaft, rotating stall) can be evaluated. The ISPC approach can be extended to deal with the effects of unshrouded stator tip clearances and stator shroud seal leakage flow, but the results were not available for this paper.

The inputs to the model are the compressor geometry, an axisymmetric compressor characteristic, and the sensitivity of the compressor characteristic to changes in axisymmetric rotor tip clearance, which are matched to data.

3.3 Two-Coupled-Actuator-Disk Model. Song and Cho [8] have developed a procedure, referred to as the two-coupled-actuator-disk model (2CAD) following the same approach used for turbines by Song and Martinez-Sanchez [9]. The 2CAD model is quasi-three-dimensional and consists of two coupled actuator-disk analyses: one at the compressor blade scale and another at the compressor radius scale. The analyses assume inviscid, incompressible flow. They are essentially mean-line analyses, and the blading is assumed to be two dimensional. The blade scale model is an axisymmetric, meridional plane analysis, and thus captures the radial redistribution of the flow due to the existence of rotor and stator tip clearances. Upon passing through a blade row, the initially radial-uniform upstream flow is assumed to split into two streams, one stream associated with the tip clearance and the remainder associated with the blade. Thus, the model can be used to examine radial flow redistribution as well as performance degradation due to rotor and stator tip clearances.

In the radius-scale analysis, the effects of nonaxisymmetric rotor and stator tip clearances can be examined. The continuity equation and the axial and tangential momentum equations are used to analyze upstream and downstream flows, and the results from the blade scale model are used to connect upstream and downstream flows. The nonaxisymmetric flow response or azimuthal flow redistribution effect is obtained through a small perturbation harmonic analysis about the axisymmetric mean, which is provided by the blade scale analysis.

Inputs required for the models are the blade angles, pitch/chord ratio, and mean rotor and stator tip clearances. Thus, no empirical inputs are needed, and the analysis is strictly based on first principles. Outputs from the model include the axisymmetric mean and nonaxisymmetric perturbations in the flow field (i.e., velocity and pressure). The nonuniform rotor blade loading effects and the effects of nonaxisymmetric static pressure on the rotor hub can be examined from the perturbations.

Assessment of the Ability of the Three Models to Compute the β Coefficient

4.1 Identification of the Roles of the Rotor Tip Clearance and the Stator Shroud Seal Effects. The first calculations of the β coefficient were done using Ehrich's 2SPC parallel compressor model in the manner reported previously [5]. The axisymmetric experimental data from Fig. 6 in Part I were used to construct a parallel compressor with one-half of the compressor operating at the nominal rotor blade tip clearance and nominal stator seal clearance, and the other half operating at open rotor blade tip clearance and nominal stator seal clearance. The results from the 2SPC model gave values of the β coefficient that were about one-half of those computed from the experimental data and suggested that a major component of the dynamic force on the rotor blade had not been identified in the analysis.

To help understand this situation, we looked at a key finding from the analysis of the experimental results—a contour map of the dynamic differential pressure across the blade surface as it passed through the point of peak dynamic load for a very highly loaded operating point as shown in Fig. 1. That perspective revealed *two* intense concentrations of dynamic activity: one in the

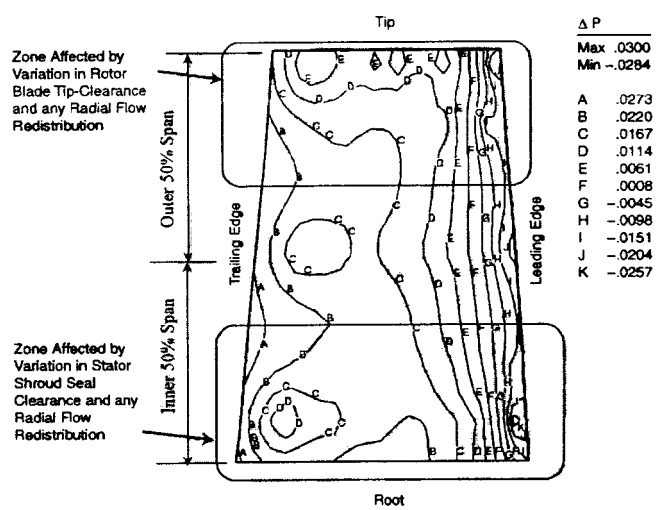

Fig. 1 Measured unsteady static pressure difference (pressure side−suction side) on the surface of the rotor blade at the minimum clearance condition for the maximum centerline offset: LSRC Compressor A

Downloaded From: http://turbomachinery.asmedigitalcollection.asme.org/ on 10/24/2016 Terms of Use: http://www.asme.org/about-asme/terms-of-use

outer one-third span of the blade surface and the other in the *inner* one-third span. It was hypothesized (and ultimately verified in the following analyses) that the activity in the outer one-third span resulted from the variation in *rotor-blade* tip clearance induced by the rotor offset as seen by a typical rotor blade in the course of its rotation. The additional zone of intense activity in the inner one-third span was comparable in magnitude to the activity near the tip and was inferred to result from the variation in flow leakage from the *stator-shroud* seal clearance as seen by the rotating blade. Although the effect of stator shroud-seal leakage on turbomachinery aerodynamic performance has been documented [10,11] the contribution of this phenomenon to rotor whirl instabilities had not been previously recognized in the analysis of experimental data or accommodated in analytic modeling of the problem. It became apparent that the influence of the flow leakage from the seal tooth clearance in the adjacent stator rows (and perhaps radial redistribution of flow) had a substantial impact on the dynamic forces on a rotor.

To identify the relative contributions of each of the two effects, we reduced the experimental unsteady-pressure data in terms of two separate components.

(*a*) A computation of the component of the β coefficient involving integration of the dynamic pressures over the outer 50 percent span of the rotor blade, representative of the cross-coupled forces derived from the variation of rotor-blade tip clearance seen by the rotating blade.

(*b*) A computation of the component of the β coefficient involving integration of the dynamic pressures over the inner 50 percent span of the rotor blade, representative of the cross-coupled forces derived from the variation of stator-shroud seal tooth clearance seen by the rotating blade.

The total value of the experimental β coefficient was then taken as the sum of these two contributions. It represented the cross-coupled forces derived from the variation of both the rotor-blade and stator-shroud seal clearances seen by the rotating blade. The two components of the β coefficient computed above and their sum are presented in Fig. 2.

With this compartmentalization of the individual effects, it was then possible to compare the experimental results with those obtained from three different analytic models.

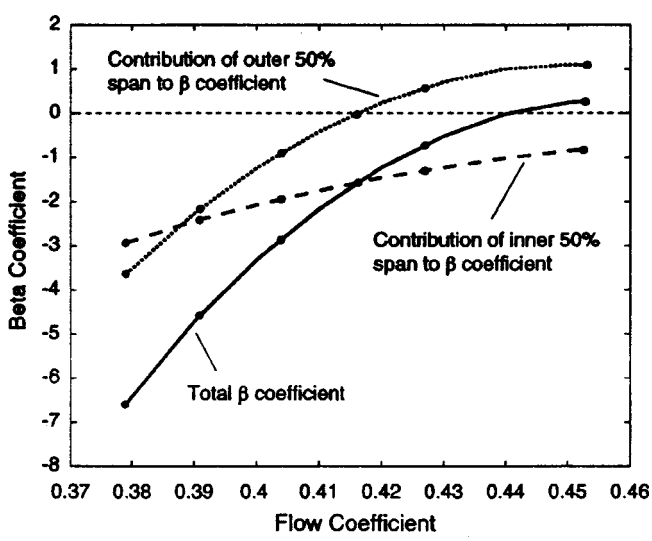

Fig. 2 Relative contributions to the total β coefficient obtained from the experimental data for inner 50 percent and outer 50 percent spans compared to the total β coefficient: LSRC Compressor A

4.2 Calculation of the β Coefficient Using the Three Models

Two-Sector-Parallel-Compressor Model. The 2SPC analytic model was exercised to produce an estimate of the two β coefficients implicit in Compressor A (described in Part I) in the following two-step process.

First, the β coefficient associated with the variation of rotor-blade tip clearance was computed from two of the sets of LSRC data (Fig. 6 of Part I): one set at nominal rotor-blade tip clearance and nominal stator-seal clearance and the other set at open rotor-blade tip clearance and nominal stator-seal clearance. These 2SPC analytic results are compared to offset rotor experimental data integrated over the outer 50 percent span in Fig. 3(*a*). The model predicts the β coefficient to an accuracy of 0.78, with a confidence level of 95 percent.

Secondly, the β coefficient associated with the variation of stator shroud seal clearance was also computed from two of the sets of LSRC data (Fig. 6 of Part I): one set at nominal rotor-blade tip clearance and nominal stator-seal clearance and the other set at nominal rotor-blade tip clearance and open stator-seal clearance. These 2SPC analytic results are compared to offset rotor experi-

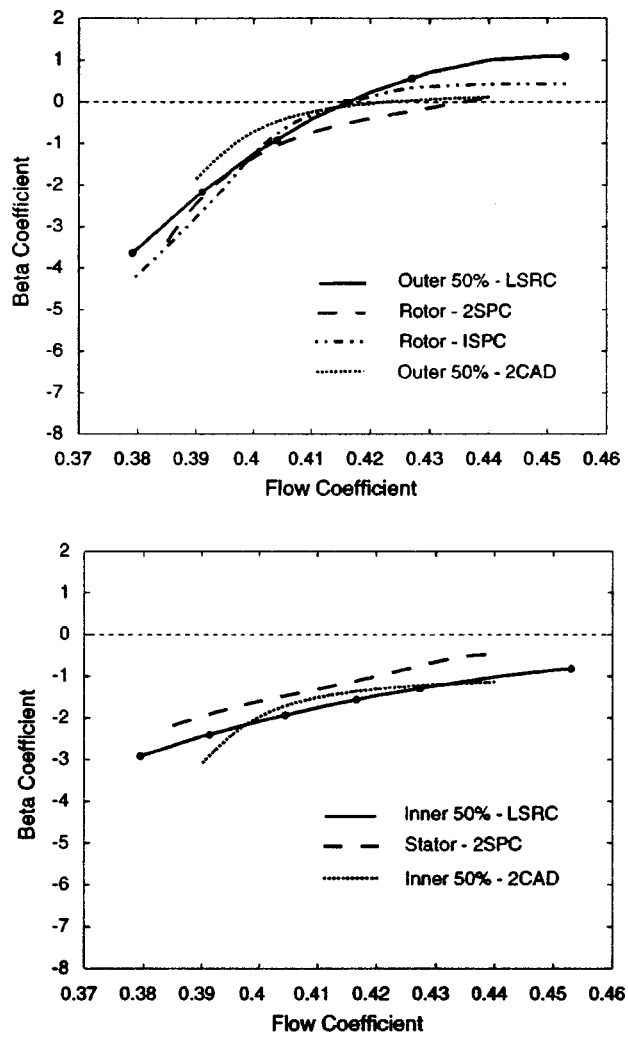

Fig. 3 Alford β coefficient for LSRC centerline offset of Compressor A. (*a*) Pressure integration over outer 50 percent span compared with analytic models of rotor-blade tip clearance effect. (*b*) Pressure integration over inner 50 percent span compared with analytic models of stator-shroud seal clearance effect.

Downloaded From: http://turbomachinery.asmedigitalcollection.asme.org/ on 10/24/2016 Terms of Use: http://www.asme.org/about-asme/terms-of-use

mental data integrated over the inner 50 percent span in Fig. 3(*b*). The model predicts the β coefficient to an accuracy of 0.51, with a confidence level of 95 percent.

Figure 4 shows the *sum* of these two effects derived from the 2SPC model compared to the offset rotor experimental data integrated over the entire 100 percent span of the rotor blade. The analytic model results agree precisely in form and yield an accuracy of 0.62 (with a confidence level of 95 percent), thus validating the 2SPC model for this general type of compressor blading.

Infinite-Segment-Parallel-Compressor Model. The ISPC compressor model was used to assess the effect of rotor-blade tip clearance on Compressor A performance. The flow field and compressor performance were computed for a steady shaft offset of 0.9 percent tip clearance to chord and different throttle settings. The performance predictions by the ISPC model and the measured mean operating points are shown in Fig. 5 compared to the experimental data. In addition the locus of operating points around the circumference is marked for one operating point by the lightly dashed line. Although only the sensitivity of the compressor characteristic to changes in axisymmetric rotor tip clearance is used in the model, the average performance predictions match the offset data quite well.

These results in Fig. 5 give confidence in using this flow field to predict the forces on the rotor. The estimate of the β coefficient from the ISPC model for the effect of rotor-blade tip clearance is shown in Fig. 3(*a*) compared to the results derived from the LSRC centerline offset experiment for Compressor A. The model predicts the β coefficient to an accuracy of 0.47, with a confidence level of 95 percent.

Two-Coupled-Actuator-Disk Model. The 2CAD model was used to predict the rotor blade loading with both rotor and stator clearances. The resultant β coefficient for the outer 50 percent rotor blade span is plotted versus flow coefficient in Fig. 3(*a*), and the resultant β coefficient for the inner 50 percent rotor blade span is plotted in Fig. 3(*b*). The model predictions yield an accuracy of 1.08 and 0.39 respectively, with a confidence level of 95 percent. Finally, the combined effects are shown in Fig. 4. The results reflect an accuracy of 1.12 with a confidence level of 95 percent. The 2CAD model assumes an unshrouded stator with a tip clearance, when, in fact, the LSRC has a single-tooth labyrinth seal on the shrouded stator tip. Nevertheless, the agreement between the 2CAD prediction and the experimental data is remarkable. Even though it might be fortuitous, the result is quite creditable considering that, as distinct from the 2SPC and ISPC models, no experimental stage characteristics or sensitivities were used in its generation.

4.3 Use of the 2SPC Model to Analyze other Compressor Configurations. With the validation of the 2SPC method by the assessment shown in Sec. 4.2, it appeared to be justified to apply the analysis tool to other axial-flow compressors for which data were available. As shown in Fig. 9 of Part I of this paper, stage performance for Compressor B (typical of modern designs having high hub/tip ratio, low aspect ratio, high-solidity blading, and shrouded stators) and Compressor C (with cantilevered stators and blading with lower hub-tip ratios and higher aspect ratios) was available from LSRC models similar to that shown for Compressor A in Fig. 6 of Part I of this paper. Both axial-flow compressors are in actual commercial airline service. Performance was in the form of overall stage-average pressure characteristics measured at two different values of both axisymmetric rotor tip clearance and stator shroud-seal clearance for Compressor B and two different

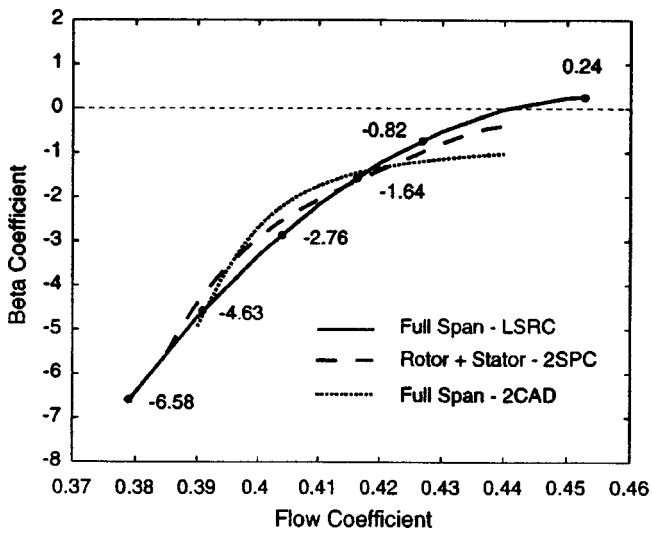

Fig. 4 β coefficient for LSRC centerline offset of Compressor A with pressure integration over entire rotor span compared with analytic models of the sum of rotor-tip and stator-shroud seal clearance effects

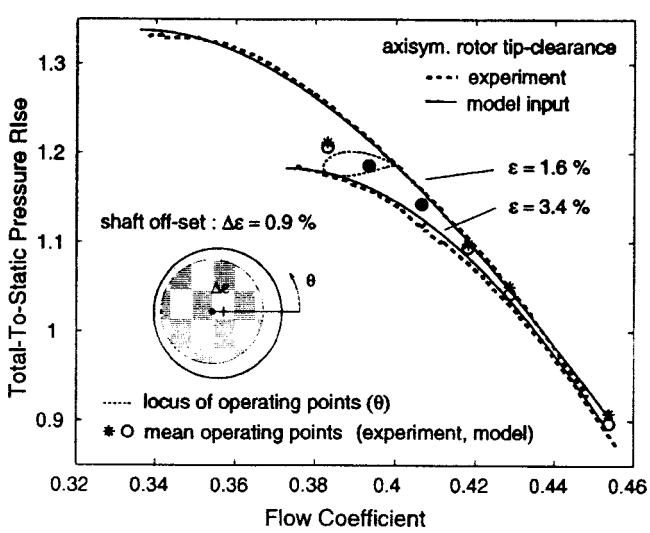

Fig. 5 Compressor A performance predictions by the ISPC model compared with experimental performance data of the LSRC

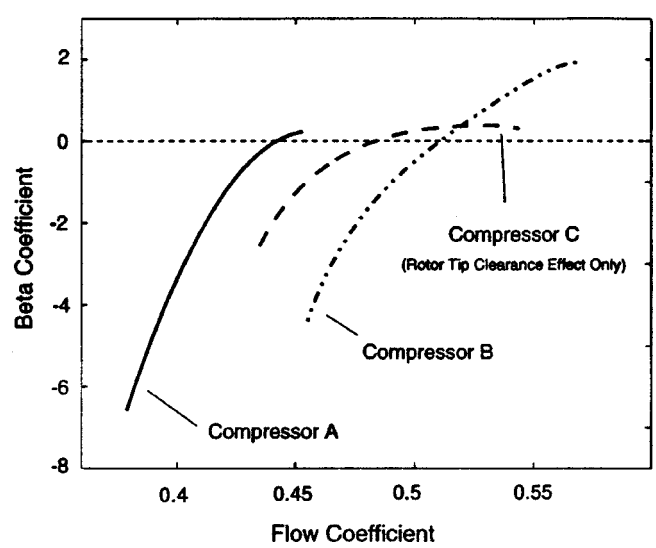

Fig. 6 β coefficient for LSRC Compressors A, B, and C using the 2SPC method, reflecting rotor and stator tip clearance changes

Downloaded From: http://turbomachinery.asmedigitalcollection.asme.org/ on 10/24/2016 Terms of Use: http://www.asme.org/about-asme/terms-of-use

values of rotor tip clearance for Compressor C. The results for Compressors B and C are shown in Fig. 6 compared with the results obtained for Compressor A. They suggest that the trends, magnitude, and sign of the predicted values of the β coefficients conform to the generality derived from the experiments for Compressor A but that detailed analysis is required for each compressor to accommodate its specific design features.

5 Discussion of Important Additional Issues

5.1 Phase Shift between the Locations of Minimum Clearance and Maximum Tangential Force. As shown in Fig. 12 of Part I of this paper, experimental LSRC measurements for the maximum centerline offset of Compressor A operating at high loading indicate a significant phase difference of about 40 deg in the peak of the dynamic force variation relative to the vector of the rotor displacement. That is, the peak dynamic force on a given blade was not developed at the same angular location where the blade was experiencing the minimum tip gap. Both the ISPC and the 2CAD models were used to predict the dynamic force distribution for a steady shaft offset. The modeling results showed the same trends in blade loading distribution as observed in the experiment. The ISPC model and the 2CAD model predict a phase lag of 26 and 28 deg, respectively, compared to the experimental value of 40 deg. A detailed analysis using the ISPC model revealed that the flow field lags the clearance distribution due to fluid inertia in the ducts and the blade rows, which gives a shift in the tangential blade loading distribution with respect to the tip-clearance asymmetry. The reasons for this are discussed briefly using the ISPC model.

First let us assume that the family of axisymmetric tip clearance compressor characteristics has no curvature and that unsteady losses and flow inertia effects in the blade rows and ducts are neglected. In this case the flow instantaneously responds to the distortion induced by the asymmetric tip clearance. The pressure rise and flow coefficient variations are then purely sinusoidal and 180 deg out of phase with respect to the tip clearance distribution. Regions with tight tip clearance yield high pressure rise, less blockage, and therefore a higher flow coefficient. The opposite holds for regions of large tip clearance.

Now let us consider the family of compressor characteristics shown in Fig. 5 and assume that unsteady losses and unsteady flow inertia effects are present. The compressor pressure rise distribution around the annulus is now distorted due to curvature of the compressor characteristics (see lightly dashed line in Fig. 5). Part of the compressor pressure rise is now devoted to accelerating the fluid in the blade row passages. The flow coefficient variation lags the tip clearance distribution due to the fluid inertia. The combination of a simplified tangential momentum analysis and kinematic relations reveals that, to first order, the variation in tangential blade loading is proportional to the variation in flow coefficient. Hence the tangential blade loading is predicted to lag the tip clearance distribution as is observed in the experiment and shown in Fig. 12 of Part I of this paper. A more detailed discussion is given in [7].

In other words, there is a finite amount of time necessary for the circulation around the rotor tip to be completely reestablished in response to the change in clearance. This time is associated with that necessary for the fluid to transverse the axial length of the rotor. However, since the tip clearance is continually changing, this is a dynamic process.

Unlike the ISPC model, the fluid inertia in the blade passage is not explicitly modeled in the 2CAD approach. Instead, the 2CAD model looks at the global flow behavior as it approaches the compressor with nonaxisymmetric flow redistribution. The phase lag of the blade loading nonuniformity relative to the tip clearance variation is mainly due to the higher mass flux near the smaller gap region. In summary the effect of flow redistribution due to inertial flow effects induces a significant phase shift (on the order of 40 deg) of the dynamic blade loading distribution.

5.2 Effect of Spool Pressure Loading. Nonaxisymmetric pressure distribution was first identified as a separate forcing source by Martinez-Sanchez et al. [12], and its effects on turbines were analyzed by Song and Martinez-Sanchez [9]. In order to assess the nature and magnitude of the nonaxisymmetric pressure effects in compressors as well, Spakovszky [7] investigated the effects of flow inertia on the destabilizing forces in a detailed analysis. The ISPC modeling results showed that the flow field lags the clearance distribution due to the fluid inertia. It is deduced that, due to this phase shift, the static pressure distribution acting on the rotor hub spool results in a net force that is not parallel to the deflection direction. The pressure force therefore has a component acting tangential to the rotor deflection and hence contributes to the cross-coupled stiffness and ultimately to the value of the β coefficient.

The static pressures acting on the spool were not measured in the experiment and a definitive comparison of the modeling results to experimental data cannot be made. However the average static pressure in the blade passage at mid-span was deduced from the blade surface measurements to obtain a rough estimate of the magnitude of the pressure nonuniformity.

The nondimensional circumferential spool pressure distribution obtained from the ISPC and 2CAD models at mid-span and the rough experimental estimate of the passage pressure nonuniformity are depicted in Fig. 7 for a compressor operating point close to stall. To be consistent with the scheme used in LSRC data reduction described in Part I, only the first spatial harmonic of the pressure distribution is considered here.

The ISPC model predicts a phase shift of 16 deg between the nonuniform spool pressure distribution and the tip clearance distribution. Regions with tight tip clearance yield less blockage and therefore a higher flow coefficient. Conserving total pressure in the upstream duct (potential flow) yields lower static pressure in the tight clearance region at the compressor face. Assuming that the flow angle from the last set of stator vanes is uniform and that the downstream duct has constant area implies a uniform static pressure distribution at the compressor exit. Hence the average of the upstream and downstream static pressure will be minimal in the tight clearance region as it is shown in Fig. 7.

The 2CAD approach predicts the same trend. Essentially higher mass flux toward the tight clearance region lowers the pressure in this region at the rotor inlet, and this nonuniform pattern persists through the stage. Thus, the average pressure acting on the rotor hub has a phase shift of 32 deg relative to the clearance distribu-

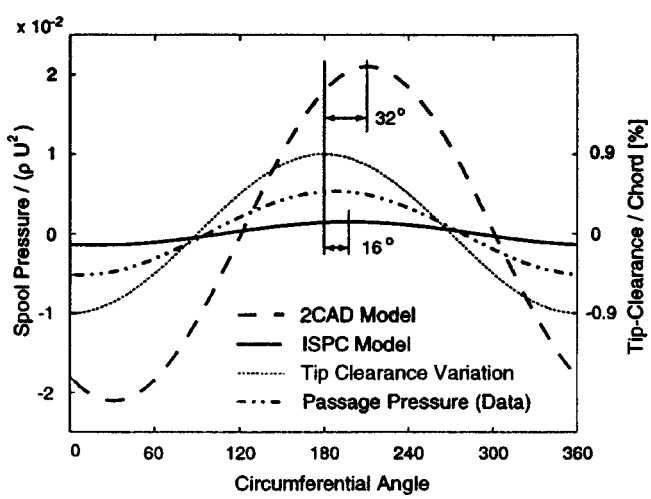

Fig. 7 The circumferential static pressure distribution obtained from the ISPC and 2CAD models at mid-span compared to experimental data

Downloaded From: http://turbomachinery.asmedigitalcollection.asme.org/ on 10/24/2016 Terms of Use: http://www.asme.org/about-asme/terms-of-use

tion. The ISPC and the 2CAD modeling results differ in the prediction of the magnitude of the pressure nonuniformity but show similar trends.

A spool loading coefficient β_{spool} equivalent in form to the β coefficient was introduced to assess the relative impact of the pressure nonuniformity. It is assumed in the calculation of the β_{spool} coefficient that the spool pressure distribution acts on the hub surface of the rotor and the adjacent upstream and downstream interblade row gaps.

The β_{spool} coefficients predicted by the ISPC and 2CAD methods are compared in Fig. 8. Both models' results show the same forward whirling trend due to the nonuniform spool pressure loading. The estimated β_{spool} coefficient acts in a direction tending to counteract the backward whirl induced by the net unbalanced tangential blade loading (see Figs. 3 and 4). The β_{spool} coefficient estimated by the 2CAD model is larger in magnitude than the ISPC prediction, which is associated with the larger magnitude and phase of the static pressure distribution in Fig. 7.

5.3 Effects of Actual Forced Rotor Whirl. The LSRC experiment was performed with a *static* offset of the rotor. In the actual situation that is being modeled, the unstable rotor would be whirling at the offset radius at the natural frequency of the system. It has been suggested that this whirling, which was not simulated in the experiment might have some significant effect on the value of the β coefficients.

Forced shaft whirl was simulated by the ISPC model to assess the effects of shaft motion on the destabilizing rotor forces (for details see [7]). (The 2CAD model can also be extended to include unsteady whirl effects as has previously been done for turbines—but that analysis was not available for this paper.) The forced whirl frequency was varied from synchronous backward whirl to synchronous forward whirl. Figure 9 provides an estimate of the impact of this effect on the β coefficient and the spool loading coefficient β_{spool}. A detailed analysis shows that an enhanced distortion of the flow field, due to shaft motion, induces an amplification of the β coefficient near a whirl frequency close to the frequency of rotating stall. The ISPC model predicts this frequency to be in the range of 22 percent to 46 percent of rotor speed for Compressor A. It should be noted that, due to the flow distortion that is generated by the shaft whirl, the rotating stall frequency varies slightly with the forced whirl frequency.

By the same token, the phase shift of the spool static pressure distribution relative to the clearance distribution varies as a function of the forced whirl frequency. The direction of induced whirl changes from forward whirl for negative frequencies to backward whirl for forced whirl frequencies above 0.1 times rotor frequency.

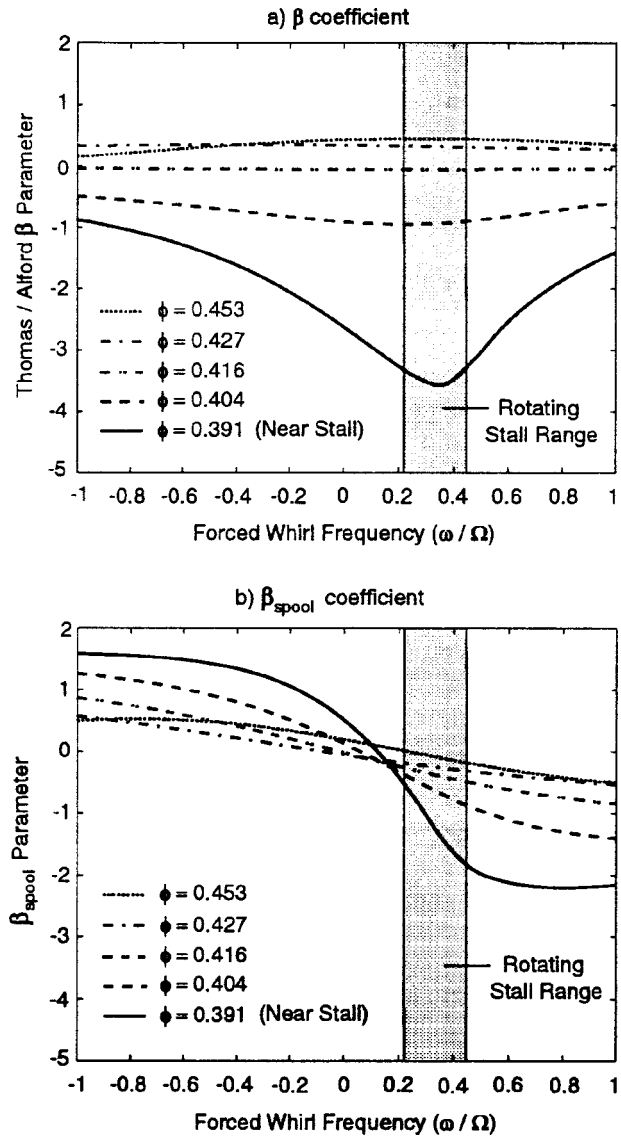

Fig. 9 β coefficient (*a*) and β_{spool} coefficient (*b*) attributable to the compressor rotor whirl effect as estimated by the ISPC model

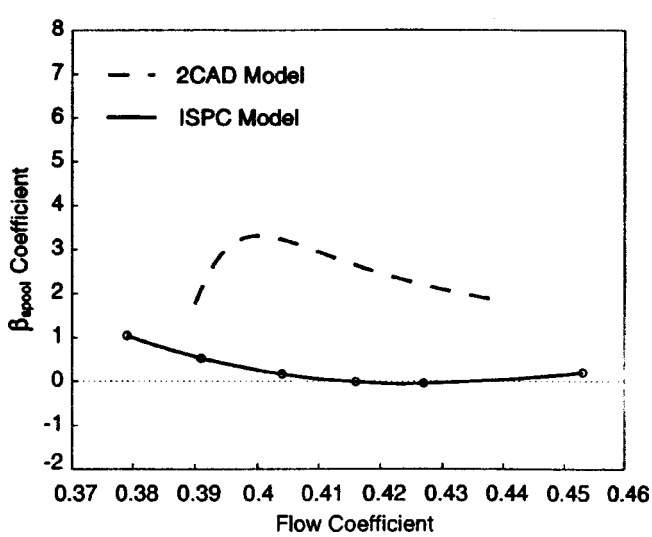

Fig. 8 Computed β coefficient attributable to the compressor spool pressure effect estimated by the ISPC and 2CAD models

It is important to note that the spool pressure-induced whirling force dampens the whirl tendency when backward whirl occurs due to the net unbalanced tangential blade loading, that is, the spool loading coefficient β_{spool} increases when the whirl frequency grows in the negative direction (see Fig. 9). The whirl speed at which the β coefficient is most affected by whirl and the angular speed of rotating stall are nearly equal. This suggests that, in an engine where the rotordynamics and compressor aerodynamics form one dynamic system, shaft whirl might interact and resonate with flow instability patterns such as rotating stall.

In summary, the simulation results from the ISPC model for actual forced rotor whirl suggest the following two important effects, which are present in actual rotor whirl but absent in our tests simulating whirl with a static offset.

1 For low flow coefficients (i.e., those near stall), shaft whirl close to rotating stall frequency enhances backward whirl, which implies a more negative β coefficient, as seen in Fig. 9(*a*). At the

Downloaded From: http://turbomachinery.asmedigitalcollection.asme.org/ on 10/24/2016 Terms of Use: http://www.asme.org/about-asme/terms-of-use

other flow coefficients shown in Fig. 9(*a*), the additional contributions to the β coefficient of actual rotor whirl are relatively small and constant.

2 As forced whirl frequency changes from synchronous backward whirl (negative frequencies in Fig. 9(*b*)) to synchronous forward whirl (positive frequencies in Fig. 9(*b*)), the sign of the β_{spool} coefficient changes from positive to negative. This implies that the spool pressure effect dampens the whirling motion.

An additional finding for a statically deflected rotor is the existence of a relatively small contribution (compared to the total β coefficient) originating from the action of asymmetric pressure forces on the spool; this contribution tends to oppose that of the blading itself.

6 Capability of the Three Models

• The 2SPC method [5] gave predictions of the basic β coefficient for both the unshrouded rotor and the shrouded stator and the combined effect of the two that were accurate enough to justify their use in design calculation where the effects of nonaxisymmetric static pressure distribution on the rotor spool and the effects of rotor whirl might not be important. The method is applicable to any axial-flow compressor where an experimental definition of the stage characteristics at two levels of axisymmetric clearance is available.

• The ISPC method [7] provides a much better prediction than the 2SPC method of the basic β coefficient due to rotor tip clearances. The ISPC method is not limited to evaluation of the effect of rotor tip clearance. It can also be extended to analyze stator hub clearance and seal leakage flow effects but the results were not available for this paper. The rotor force model is not limited to the particular compressor model used here: any prediction of the compressor flow field (i.e., CFD analysis, experimental data, etc.) can be used to predict the aerodynamically induced rotor forces. The ISPC method provides a means for estimating the effects of the static pressure distribution on the rotor spool and of the effects of rotor whirl and can be easily integrated in existing engine design tools, particularly where the effects of nonaxisymmetric static pressure distribution on the rotor spool and the effects of rotor whirl may be important.

• The 2CAD method [8] does not require any prior experimental definition of stage characteristics and so is capable of carrying out systematic studies of the effects of stage design parameters to ascertain their influence on rotordynamic instability without requiring extensive experimental stage performance data. In addition to the blade loading variation, the model can predict nonaxisymmetric static pressure distribution on the rotor spool. Although not included in this paper the 2CAD method can be extended to accommodate rotor and stator shrouds (i.e., seals) and unsteady whirl effects.

7 Conclusions

This is the first time that definitive measurements, coupled with compelling analyses, have been reported in the literature to resolve whirl instability issues important in the design of modern, axial-flow compressors.

1 The computation of the β coefficient from all three models assessed in this paper showed agreement when compared to the experimental data in both form and direction, thus validating their use to understand whirl effects in compressors. In addition, the validation provides confidence for designers to use the models in the assessment of rotordynamically stable turbomachinery.

2 All three analysis methods conclude that the Thomas/Alford forces generally promote *backward* rotor whirl (associated with negative β coefficient) except for operation at higher flows where the results were mixed, with some compressors having strongly negative β and others having β's near zero or slightly positive. At lower-flow conditions, the β's were generally strongly negative.

3 It was established that the effects of rotor tip clearance explain only about one-half of the total value of the β coefficient. It is necessary to recognize the influence of the flow leakage around the stator-shroud seal-tooth clearance to understand and account for the full effect.

4 The ISPC model gave additional insight into the effects of an actual forced rotor whirl, which were not modeled in the experiment. For low flow coefficients (i.e., those near stall), shaft whirl close to rotating stall frequency enhances backward whirl, which implies a more negative β coefficient. At the other flow coefficients the additional contributions of actual rotor whirl to the β coefficient are relatively small and constant.

5 The modeling results are not definitive for the effect of nonaxisymmetric spool pressure distribution on the β coefficient. The ISPC model suggests that, for static shaft deflections, β_{spool} is quite small at flow coefficients typical of the operating regime of this class of compressors. The 2CAD model suggests that the effect of nonaxisymmetric spool pressure distribution may be more significant than predicted by the ISPC model. For forced shaft whirl β_{spool} is of comparable magnitude to the β coefficient (rotor effect only). It opposes the effects of the β coefficient for two cases: for negative whirl frequencies and low flow coefficients and for positive whirl frequencies and high flow coefficients.

6 The validated computational capability described above provides the general means to predict the aerodynamic destabilizing forces for axial-flow compressors in gas turbine engines (subject to the limitations that might result from the approximations implicit in the analytic models where the effects of compressibility and variations in radius ratio were not addressed). This capability permits improved accuracy in predicting the rotordynamic instability thresholds for existing, derivative, and new turbomachinery designs that will operate at higher speeds and higher energy-density levels in the future.

References

[1] Thomas, H. J., 1958, ''Unstable Natural Vibration of Turbine Rotors Induced by the Clearance Flow in Glands and Blading,'' Bull. AIM, **71**, No. 11/12, pp. 1039–1063.

[2] Alford, J., 1965, ''Protecting Turbomachinery From Self-Excited Rotor Whirl,'' J. Eng. Power, Oct., pp. 333–334.

[3] Vance, J. M., and Laudadio, F. J., 1984, ''Experimental Measurement of Alford's Force in Axial Flow Turbomachinery,'' ASME J. Eng. Gas Turbines Power, **106**, No. 3, pp. 585–590.

[4] Colding-Jorgensen, J., 1992, ''Prediction of Rotordynamic Destabilizing Forces in Axial Flow Compressors,'' J. Fluids Eng., **114**, No. 4, pp. 621–625.

[5] Ehrich, F. F., 1993, ''Rotor Whirl Forces Induced by the Tip Clearance Effect in Axial Flow Compressors,'' J. Vibr. Acoust., **115**, pp. 509–515.

[6] Yan, L., Hong, J., Li, Q., Zhu, Z., and Zhao, Z., 1995, ''Blade Tip Destabilizing Force and Instability Analyses for Axial Rotors of Compressor,'' AIAA Paper No. A95-40315, Beijing University of Aeronautics and Astronautics, Beijing, China.

[7] Spakovszky, Z. S., 2000, ''Analysis of Aerodynamically Induced Whirling Forces in Axial Flow Compressors,'' ASME J. Turbomach., **122**, No. 4, pp. 761–768.

[8] Song, S. J., and Cho, S. H., 2000, ''Non-uniform Flow in a Compressor D Asymmetric Tip Clearance,'' ASME J. Turbomach., **122**, pp. 751–760.

[9] Song, S. J., and Martinez-Sanchez, M., 1997, ''Rotordynamic Forces Due to Turbine Rip Leakage,'' ASME J. Turbomach., **119**, No. 3, pp. 695–713.

[10] Wisler, D. C., 1985, ''Loss Reduction in Axial-Flow Compressors Through Low-Speed Model Testing,'' ASME J. Eng. Gas Turbines Power, **107**, pp. 354–363.

[11] Wellborn, S. R., and Okiishi, T. H., 1999, ''Influence of Shrouded Stator Cavity Flows on Multistage Compressor Performance,'' ASME J. Turbomach., **121**, No. 3, pp. 486–498.

[12] Martinez-Sanchez, M., Jaroux, B., Song, S. J., and Yoo, S. M., 1995, ''Measurement of Tip Blade–Tip Rotordynamic Excitation Forces,'' ASME J. Turbomach., **117**, No. 3, pp. 384–392.

Downloaded From: http://turbomachinery.asmedigitalcollection.asme.org/ on 10/24/2016 Terms of Use: http://www.asme.org/about-asme/terms-of-use